Sol-gel preparation and spectroscopic study of the pyrophanite $MnTiO_3$ nanoparticles

ZHOU Guowei[1], KANG Youngsoo[2], LI Tianduo[1] & XU Guiying[3]

1. School of Light Chemicals and Environmental Engineering, Shandong Institute of Light Industry, Jinan 250100, China;
2. Department of Chemistry, Pukyong National University, Daeyeon-3-dong, Nam-gu, Pusan 608-737, Korea;
3. Key Laboratory for Colloid and Interface of Ministry of Education of China, Shandong University, Jinan 250100, China
Correspondence should be addressed to Zhou Guowei (email: guoweizhou@hotmail.com)

Received November 11, 2004

Abstract The nanosized xerogel of titanium dioxide (TiO_2) and manganese oxides (MnO_2, Mn_2O_3, Mn_3O_4) was prepared by the sol-gel method using manganese chloride ($MnCl_2 \cdot 4H_2O$) and titanium isopropoxide ($Ti(O\text{-}iPr)_4$) as precursors in cetyltrimethylammonium bromide (CTAB)/ethanol/H_2O/HCl micelle solutions, following the calcinations of the produced powders at difference temperatures. The nanostructure and phase composition of these nanoparticles were characterized with X-ray powder diffraction (XRD), transmission electron microscopy (TEM), energy dispersive X-ray spectroscopy (EDX) and X-ray photoelectron spectroscopy (XPS). The spectroscopic characterizations of these nanoparticles were also done with UV-Vis spectroscopy and laser Raman spectroscopy (LRS). XRD patterns show that the pyrophanite $MnTiO_3$ phase was formed at the calcinations temperature of 900℃. The TEM images show that the nanoparticles are almost spherical or slight ellipose and the sizes are 50 nm on average. The UV-Vis spectra show that the nanosized $MnTiO_3$ have significant absorption bands in the visible region. There are new absorption peaks of $MnTiO_3$ nanoparticles in LRS compared with the pure TiO_2 powder.

Keywords: pyrophanite $MnTiO_3$, nanoparticles, spectroscopy, CTAB micelle, sol-gel.

DOI: 10.1360/04yb0034

Titanium dioxide (TiO_2) is one of the green catalysts, which has attracted much attention due to its promising applications in the purification of air, the bactericidal action of water, and environmental photocatalytic degradation of organic pollutant compounds in waste water[1,2]. TiO_2 includes three phases: brookite, antase and rutile. The effective photoexcitation of TiO_2 semiconductor particles requires the application of light with energy higher than the titania band gap energy (E_{bg}). The band gap energy of TiO_2 is about 3.2 eV for anatase and 3.02 eV for rutile, therefore the absorption thresholds correspond to 380 and 410 nm for the two titania forms, respectively. Thus, if natural sunlight should be used for the photoexcitation of this material, only the ultraviolet fraction (about 5%) of the solar irradiation has sufficient energy for this process. It is believed that the extension of light absorption can improve photocatalytic activity of semiconductor. A possibility to overcome this obstacle is doping numerous ions like noble metals, transition metals into the titanium dioxide to change the absorption band to a visible range. The effect of doping is to change the equilibrium concentration of electrons or holes, and the light absorption band of metal-TiO_2 can

be shifted into the visible region[3]. In transition metal, manganese acts as efficient catalyst in many industrially important oxidation processes, due to its variable oxidation states (+2, +3, +4 and +7).

In recent years, Ding[4] and Gallardo-Amores[5] reported the synthesis and photocatalystic properties of TiO_2-MnO, TiO_2-MnO_2 composite nanomaterials. We have prepared the $MnTiO_3$ nanoparticles using commercial TiO_2 and $MnCl_2{\cdot}4H_2O$ as base materials[6]. The objective of this paper is to investigate the synthesis of pyrophanite $MnTiO_3$ nanoparticles. It was produced by calcinations of xerogel of TiO_2 and manganese oxide (MnO_2, Mn_2O_3, Mn_3O_4), which was prepared by the sol-gel method using manganese chloride ($MnCl_2{\cdot}4H_2O$) and titanium isopropoxide ($Ti(O\text{-}iPr)_4$) as base material in CTAB/ethanol/H_2O/HCl micelle solutions. The structure and spectroscopic properties of nanoparticles were investigated.

1 Experimental

1.1 Materials

Cetyltrimethylammonium bromide (CTAB), titanium isopropoxide ($Ti(O\text{-}iPr)_4$) and manganese chloride tetrahydrate ($MnCl_2{\cdot}4H_2O$) were purchased from Aldrich Chemical Co. and were used as received. Titanium dioxide powder P-25, which is predominantly anatase (70% anatase, 30% rutile), was purchased from Degussa Co. (Germany) and was used without any further treatment. The other materials were of analytical grade and used as produced without further purification. Distilled water was used throughout this study.

1.2 Preparation of $MnTiO_3$ nanoparticles

A typical synthesis procedure is as follows: first, the mixture of distilled water with ethanol, HCl and $MnCl_2{\cdot}4H_2O$, was put in reflux at 70℃ and stirred constantly for 30 min; second, the mixed solution of CTAB and ethanol was added; third, $Ti(O\text{-}iPr)_4$ was added drop by drop to the above mixture while refluxing, and then the solution was further refluxed for 12 h at 70℃; finally, the resulting solution was left to an open container at 70℃ until the xerogel was formed upon solvent evaporation. This method gives a $MnCl_2/Ti(O\text{-}iPr)_4$ molar ratio of 1.00, CTAB/$Ti(O\text{-}iPr)_4$ molar ratio of 0.20, water/$Ti(O\text{-}iPr)_4$ molar ratio of 17.00, hydrochloric acid/$Ti(O\text{-}iPr)_4$ molar ratio of 1.40, ethanol/$Ti(O\text{-}iPr)_4$ molar ratio of 20.00. The xerogel was dried in air at 100℃ for 12 h, ground to fine powder and calcined in air at 600, 700, 800, 900℃ for 6 h, respectively.

1.3 Characterization techniques

To investigate the phase composition and the crystallite size distribution of the nanoparticles after the calcinations, X-ray powder diffraction (XRD) measurement was performed. XRD patterns were recorded on a Philips X'pert-MPD diffractometer, using Cu Kα radiation, The crystallite sizes were calculated from the peak widths using the Scherrer equation. The transmission electron microscopy (TEM) studies were carried out with a JEOL JEM2010 transmission electron microscope. Semiquantitative analyses were carried out on an energy-dispersive X-ray (EDX) spectroscopy spectrometer connected to a Hitachi S-2400 Scanning Electron Microscope. X-ray photoelectron spectroscopy (XPS) studies were performed with a Vacuum Generators photoelectron spectrometer (VG-Scientific ESCALAB 250 spectrometer) with monocromatized Al Kα X-ray source. The C1s signal (285 eV) was taken as an internal standard to calculate the binding energies (E_b). The UV-Vis absorption spectra were obtained with a Varian Cary 1C UV-Visible spectrophotometer. The samples were ultrasonically dispersed in distilled water at 10^{-4} mol·L^{-1} for 30 min. Raman spectra were recorded with a BRUKER (Germany) FRA-106/S spectrometer, using the 1064 nm excitation line of Nd-YAG Laser. The data were collected by keeping the power at 50 mW, 100 scans and 4 cm^{-1} resolution.

2 Results and discussion

2.1 Preparation of $MnTiO_3$ nanoparticles

The oil-in-water (O/W) micelle could be formed by CTAB cationic surfactant in water, ethanol, HCl mix solutions[7]. Micelle formation is greatly affected by

short-chain alcohol present in sol-gel procedures. The hydrolysis and condensation processes of titanium isopropoxide can be efficiently controlled by adding hydrochloride acid. In the presence of surfactant micelle solution, Mn^{2+} ions react with oxygen faster and more completely and can be readily oxidized to Mn^{3+} and Mn^{4+} ions. When the reaction is done in air, the mixture of MnO_2, Mn_2O_3 or Mn_3O_4 can be formed[8,9]. The crystallite size of TiO_2 produced from hydrolysis and condensation processes of titanium isopropoxide, and MnO_2, Mn_2O_3 or Mn_3O_4 produced from the oxidation of Mn^{2+}, was controlled by the concentration of CTAB[8]. The pyrophanite $MnTiO_3$ compounds must have been produced from the reaction of the mixed manganese oxidation states with titanium dioxide during the decomposition of CTAB in the certain temperature calcinations process[5]:

$$Mn_2O_3 + 2TiO_2 \rightarrow 2MnTiO_3 + 0.5O_2 \quad (1)$$

$$Mn_3O_4 + 3TiO_2 \rightarrow 3MnTiO_3 + 0.5O_2 \quad (2)$$

$$MnO_2 + TiO_2 \rightarrow MnTiO_3 + 0.5O_2 \quad (3)$$

2.2 XRD patterns

In order to analyze the crystal phases, XRD patterns were recorded. The obtained XRD patterns of xerogel of manganese oxides and titanium dioxide at different calcinations temperature are shown in Fig. 1. The diffraction line is well defined and compared favorably to JCPDS card No. 77-1858 ($MnTiO_3$), 44- 0141 (MnO_2), 78-0390 (Mn_2O_3), 80-0382 (Mn_3O_4) in the products. It can be seen that the rutile phase is predominant and Mn_2O_3 is the majority of the mixture manganese oxidation states at 600, 700 and 800℃. The XRD peaks of powder calcined at higher temperature 900℃ are very different from those of the samples at 600, 700 and 800℃, which suggests a significant formation of $MnTiO_3$ at 900℃ from the reaction of MnO_2, Mn_2O_3 or Mn_3O_4 with TiO_2. This result agrees with the analysis of sec. 2.1. Gallardo-Amores et al.[5] have already reported that pyrophanite could be produced from TiO_2-supported Mn oxide XMn- TiO_2 (with X = 0.5, 1.0, 1.5 and 2.0) at 930℃. The crystal size calculated from Scherre equation by means of XRD line broadening analysis data was 57 nm.

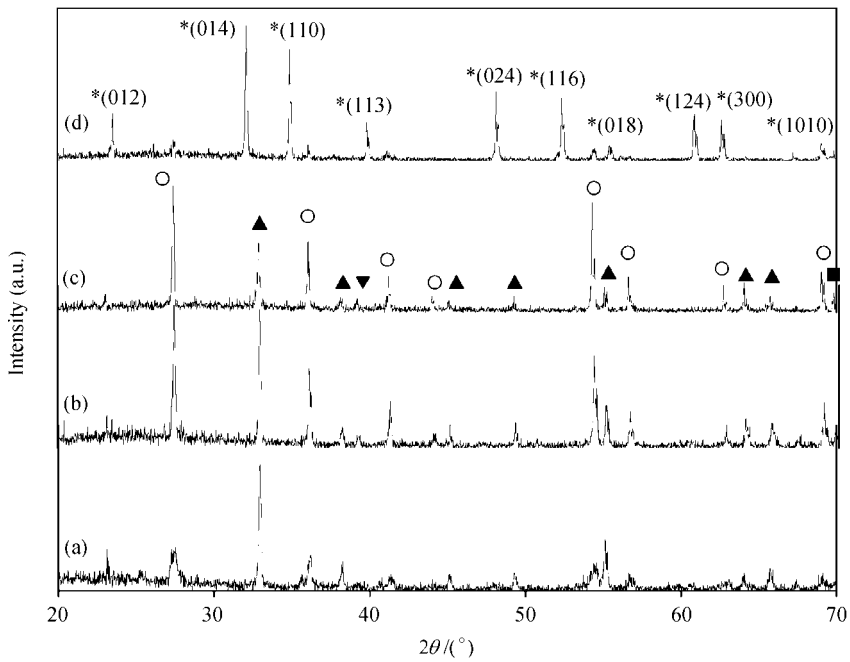

Fig. 1. XRD patterns of as-synthesized manganese oxides-TiO_2 calcined at various temperature (a) 600℃, (b) 700℃, (c) 800℃ and (d) 900℃. Peaks corresponding to $MnTiO_3$, Mn_2O_3, Mn_3O_4, MnO_2 and rutile phase are marked by *, ▲, ▼, ■ and ○, respectively.

2.3 TEM and EDX studies

TEM was performed to examine the particle size and morphology of the synthesized particles. TEM images of the xerogel of manganese oxides and titanium dioxide at the calcinations temperature of (a) 600 and (b) 900℃ are shown in Fig. 2. According to the result of XRD patterns in sec. 2.2, the production is the mixture of manganese oxides and titanium dioxide at 600℃, so the particle size is small this time. The production is new pyrophanite MnTiO3 at 900℃, so the particle size is big at this temperature, the average diameter is 50 nm. The stoichiometry of the obtained $MnTiO_3$ powder was demonstrated by EDX measurement. The elemental analyses results of P-25 and $MnTiO_3$ are showed in Table 1. The results of EDX data of $MnTiO_3$ nanoparticles (O/Ti = 2.86, O/Mn = 2.79) are in agreement with the elemental mole ratio (O/Ti = 3, O/Mn = 3) in the theoretical formula of $MnTiO_3$. These also confirm that this material consists of essentially titan-oxygen-metal networks and that transition metal Mn has formed a compound with Ti to $MnTiO_3$ at 900℃.

2.4 XPS results

The Mn 2p XP spectra of xerogel at the calcinations temperature of (1) 600 and (2) 900℃ are shown in Fig. 3. The main signals of the binding energy (E_b) of Mn $2p_{3/2}$ and Mn $2p_{1/2}$ doublet are accompanied with a shoulder peak (sh) at their high-energy side. This can be interpreted in terms of ligands → transition metal charge transfers. The binding energy of Mn $2p_{3/2}$ at the calcinations temperature of 600℃, E_b (Mn $2p_{3/2}$) = 640.8 eV, is higher than E_b (Mn $2p_{3/2}$) = 640.2 eV in the MnO-TiO_2[10]. But the binding energy of Mn $2p_{3/2}$ at the calcinations temperature of 900℃, E_b (Mn $2p_{3/2}$) = 640.0 eV, is slightly lower than this data. It can be concluded that the oxidation state of Mn is above +2, existing in the form of MnO_2, Mn_2O_3 or Mn_3O_4 at 600 ℃, while the nanoparticles MnTiO3 could be formed at 900℃.

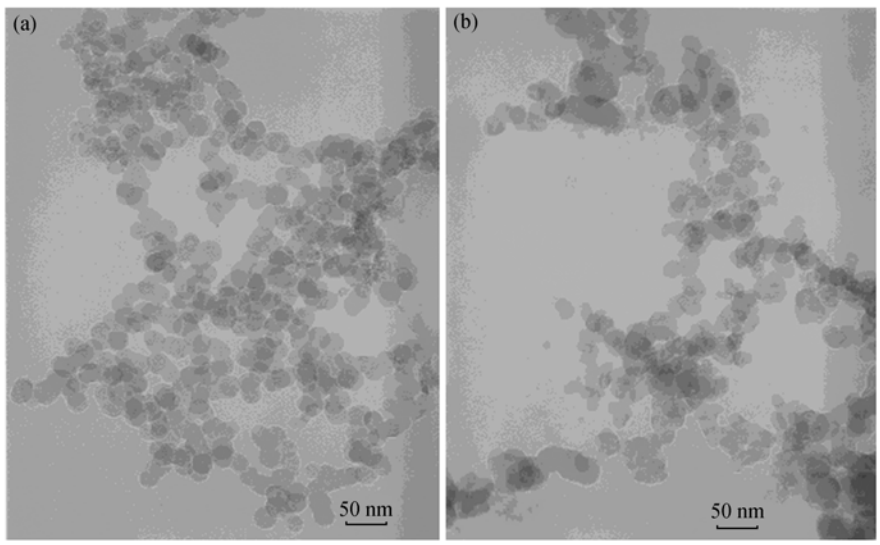

Fig. 2. TEM micrographs of as-synthesized manganese oxides-TiO_2 at different calcinations temperature (a) 600℃ and (b) 900℃.

Table 1 EDX data of xerogel at calcinations temperature 900℃

Relative elemental composition (wt%)			Relative elemental composition (atomic%)			Elemental mole ratio	
O	Ti	Mn	O	Ti	Mn	O/Ti	O/Mn
30.48	31.95	37.56	58.51	20.49	21.00	2.86	2.79

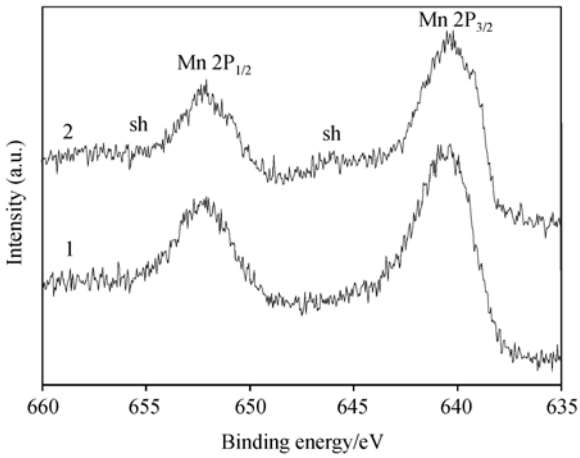

Fig. 3. XP spectra of Mn 2p at calcinations temperature (1) 600℃ and (2) 900℃.

2.5 UV-Visible spectra

UV-Vis spectra for P-25 powder and $MnTiO_3$ are shown in Fig. 4. UV-Vis spectrum of P-25 powder can be characterized with an absorption band at the wavelength of 250—320 nm as shown in Fig. 4(1). The strong absorption in the UV range is due to TiO_2 interband transitions (valence band → conduction band). The λ_{max} appearing at 320 nm are related to $O^{2-} \rightarrow Ti^{4+}$ charge transfer transitions. The UV-Vis spectra of $MnTiO_3$ in Fig. 4(2) show a wide absorption band in the wavelength of 300—700 nm. The absorption bands in the region of 300—500 nm were attributed to octahedral $Mn^{2+} \rightarrow Ti^{4+}$ intervalence charge transfer. The absorption bands at the 500—700 nm interval were assigned to the $^6A_{1g} \rightarrow {}^4A_{1g}$ and $^6A_{1g} \rightarrow {}^4T_{2g}$ crystal field transition of octahedral Mn^{2+} site[11,12].

2.6 LRS studies

In recent years, Raman spectroscopy has become an increasingly valuable tool for the investigation of the nanoparticle[5,13]. The spectra of P-25 and $MnTiO_3$ nanoparticle are comparatively shown in Fig. 5. Titanium dioxide is characterized by anatase (three bands at 397, 516 and 639 cm^{-1}) and rutile (one band at 447 cm^{-1}) as shown in Fig. 5(1). According to our XRD pattern analysis, the crystallize phases are mainly composed of manganese oxides with titanium dioxide at the calcinations temperature of 600, 700 and 800℃. So the intensity of these four peaks falls strongly down. But in the formation of $MnTiO_3$ during the calcinations at 900℃, these four bands disappear and give rise to an extremely strong feature near 700 cm^{-1}, which is certainly due to a true vibrational peak. According to the presence of a center of symmetry and the "mutual exclusion rule", there should be ten Raman active modes (5Ag + 5Eg)[12, 14], but we just observe eight Raman active fundamentals (absorption at 684, 610, 462, 360, 336, 263, 235 and 202 cm^{-1} for $MnTiO_3$) as shown in Fig. 5(2). The other two Raman peaks lost can be assigned to low intensity modes or being superimposed by other ones. The most typical feature is the strong Raman mode observed near 700 cm^{-1} (684 cm^{-1}) on $MnTiO_3$. This mode arises from the highest frequency vibrational mode of MnO_6 oc-

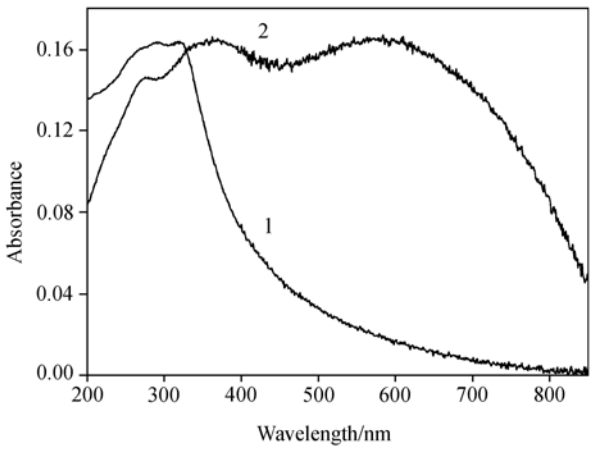

Fig. 4. UV-Vis absorption spectra of (1) P-25 and (2) pyrophanite $MnTiO_3$ nanoparticles.

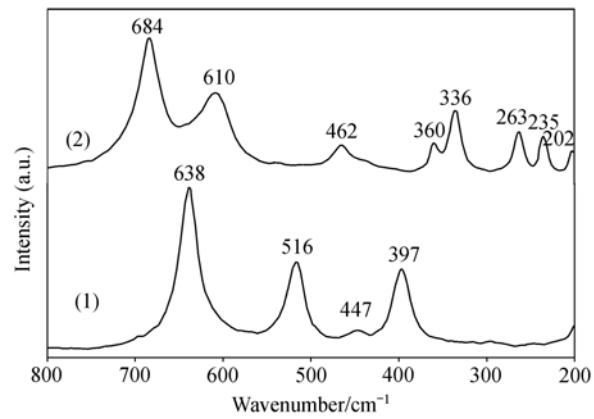

Fig. 5. Raman spectra of (1) P-25 and (2) pyrophanite $MnTiO_3$ nanoparticles.

tahedra, that is the symmetric stretching mode (A_{1g} symmetry for regular O_h octahedral)[14]. The phonon modes below 300 cm^{-1} are assigned to lattice vibrations. These also confirm the formation of $MnTiO_3$, not just the mixture of TiO_2 with manganese oxides at 900℃.

3 Conclusions

The pyrophanite $MnTiO_3$ nanoparticles can be produced from the reaction of the mixed manganese oxides with titanium dioxide in xerogel, which was prepared by the sol-gel method at 75℃ in CTAB/ ethanol/H_2O/HCl micelle solutions, during the decomposition of CTAB at the calcinations temperature of 900℃. The prepared $MnTiO_3$ nanoparticles are almost spherical or slightly stretched and the average sizes are 50 nm, showing a significant absorption band shifted into the visible region. The new Raman absorption peaks at 684, 610, 462, 360, 336, 263, 235 and 202 cm^{-1} for $MnTiO_3$ show the formation of Ti-O-Mn bonds at the calcinations temperature of 900℃, not just the mixtures of titanium dioxide with manganese oxides.

Acknowledgements This work was supported by the National Natural Science Foundation of China (Grant No. 29973023), the Key Project of Chinese Ministry of Education (No. 205088), the Scientific Research Bonus Foundation for Young and Middle-aged Scientists of Shandong Province (No. 2004BS04009) and the Foundation of Key Laboratory of Colloid and Interface Chemistry (Shandong University), Ministry of Education.

References

1. Fujishima, A., Rao, T. N., Tryk, D. A. et al., Titanium dioxide photocatalysis, J. Photochem. Photobiol. C, Photochem. Rev., 2000, 1: 1－21.
2. Ranjit, K. T., Willner, I., Bossmann, S. H. et al., Lanthanide oxide-doped titanium dioxide photocatalysts: novel photocatalysts for the enhanced degradation of p-chlorophenoxyacetic acid, Environ. Sci. Technol., 2001, 35: 1544－1549.
3. Brik, Y., Kacimi, M., Ziyad, M. et al., Titania-supported cobalt and cobalt-phosphorus catalysts: characterization and performances in ethane oxidative dehydrogenation, J. Catal., 2001, 202: 118－128.
4. Ding, S. W., Wang, L. Y., Zhang, S. Y. et al., Hydrothermal synthesis, structure and photocatalysis property of nano-TiO_2- MnO_2, Science in China, Ser. B, 2003, 46: 542－548.
5. Gallardo-Amores, J. M., Armaroli, T., Ramis, G. et al., A study of anatase-supported Mn oxide as catalysts for 2-propanol oxidation, Appl. Catal. B Environ., 1999, 22: 249－259.
6. Zhou, G. W., Kang, Y. S., Synthesis and structural properties of manganese titanate $MnTiO_3$ nanoparticle, Mater. Sci. Engineer. C, 2004, 24: 71－74.
7. Soler-Illia, G. J. de A. A., Louis, A., Sanchez, C., Synthesis and characterization of mesostructured titania-based materials through evaporation-induced self-assembly, Chem. Mater., 2002, 14: 750－759.
8. Tian, Z. R., Tong, W., Wang, J. Y. et al., Manganese oxide mesoporous structures: mixed-valent semiconducting catalysts, Science, 1997, 276: 926－929.
9. Velu, S., Shah, N., Jyothi, T. M. et al., Effect of manganese substitution on the physicochemical properties and catalytic toluene oxidation activities of Mg-Al layered double hydroxides, Microporous Mesoporous Mater., 1999, 33: 61－75.
10. Voβ, M., Borgmann, D., Wedler, G., Characterization of alumina, silica, and titania supported cobalt catalysts, J. Catal., 2002, 212: 10－21.
11. Dvoranova, D., Brezova, V., Mazur, M. et al., Investigations of metal-doped titanium dioxide photocatalysts, Appl. Catal. B Environ., 2002, 37: 91－105.
12. Carter, R. L., Molecular Symmetry and Group Theory, New York: John Wiley & Sons, 1998, 61, 208, 236.
13. Xu, C. Y., Zhang, P. X., Yan, L., Blue shift of Raman peak from coated TiO_2 nanoparticles, J. Raman Spectrosc., 2001, 32: 862－865.
14. Baraton, M. I., Busca, G., Prieto, M. C. et al., On the vibrational spectra and structure of $FeCrO_3$ and of the ilmenite-type compounds $CoTiO_3$ and $NiTiO_3$, J. Solid State Chem., 1994, 112: 9－14.